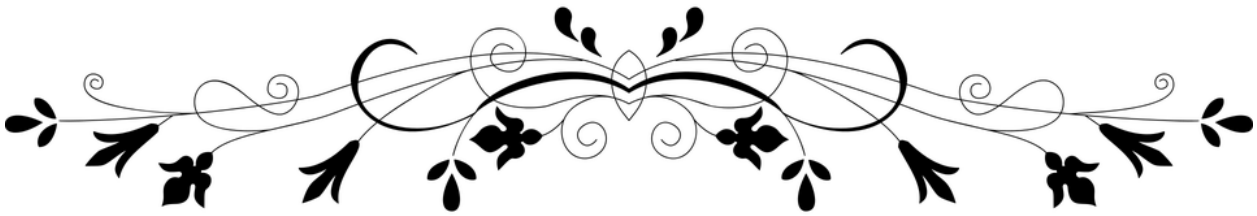

CHAPTER 5

Green Route Synthesized $NaYF_4$: Yb^{3+}, Tm^{3+} Nanophosphors and its Photophysical and Magnetic Characterization

5.1 Introduction

The issues related to effective penetration to deep lying tumor tissues, auto-fluorescence from biological cells, and environmental interference during bio-assay while using multifunctional copper based semiconducting nanostructures as a theranostic agent, could be successfully tackled by development of rare earth doped UCPs. Upconverting phosphors excited with near-infrared radiation (NIR) not only facilitates the generation of highly resolute images of deep-lying tumor tissues [347-349] having a high signal-to-noise ratio but also holds potential for augmented heat generation for advanced treatment purposes.

Trivalent thulium-doped $NaYF_4$ Upconverting host lattice having low phonon energy and chemical stability [240, 350-352] have attracted significant attention due to its strong UV and blue light emission tunable to surrounding atmosphere [177]. The violet light and blue light emanating from Tm^{3+}-Yb^{3+} co-doped $NaYF_4$ Upconverting phosphors successfully investigated for several chemical and biological processes [178]. Additionally, it also has been used for fabrication of small wavelength solid state lasers [177]. Therefore $NaYF_4$:Yb^{3+}, Tm^{3+} Upconverting phosphors are suitable candidate for development of a multifunctional system having diverse application in the field of cancer theranostics and additional physicochemical sectors like magnetism, energy harvesting etc.

The $NaYF_4$ Upconverting phosphors, exists in two phases: cubic (α) and hexagonal (β) [353] with latter being more efficient [354]. However, synthesis technique involving rapid phase transformation (α → β), improved crystallinity, tunable morphology and enhanced luminescence property remains a challenge. Further reported researches involve complex experimental setup, high decomposition temperature of organometallic

precursors, additional product purification steps [355]. Similarly, use of toxic and corrosive acids limits there possible biological usage. Nevertheless, studies incorporating synthetic long-chain saturated and unsaturated alkyl compounds (long-chain fatty acid esters) have been reported to control phase, crystallinity, and morphology of the Upconverting phosphors [202], those are abundantly available in several plant extracts [228, 230]. Thus use of plant extracts shall definitely make the synthesis process facile and environmentally friendly. During synthesis aforementioned phytochemicals chelates to the Re^{3+} ions, bond weakening of which, results in primary nucleation followed by crystal growth and stabilization. This whole process facilitates better Re^{3+} ion dispersion, leading to formation of several uniform nucleation centers, which result in generation of comparable sized nanostructures. This concept can be directly utilized to alter the phase formation, control morphology, size and other physical properties, by carefully choosing the plant extract and thereby the organic ligands.

To synthesize Yb^{3+}/Tm^{3+} co-doped Upconverting nanophosphors (UPCN), the hydrothermal route is preferable due to its low-temperature processing and simple experimental setup, unlike the high-temperature thermal decomposition, and liquid-solid two-phase methods. Moreover, hydrothermal method is an affordable technique for preparing phase pure, crystalline Upconverting phosphors [356].

Hence the objective of the current study is to synthesize Yb^{3+}-Tm^{3+} co-doped $NaYF_4$ Upconverting phosphors by suitably adapting the green route involving plant extract and examining the resulting crystallographic and morphological parameters. These are the important aspects of Upconverting system, from biological application prospective. Further it is important to examine the luminescence properties and photothermal heat

generation capability by exciting with 975 nm NIR laser aimed at diagnosing and treating tumor tissues grown deep inside the body.

5.2. Experimental

5.2.1 Synthesis of Upconverting $NaYF_4:Yb^{3+}$, Tm^{3+} Nanophosphors

The *M.oleifera* leaf extract was used for the synthesis of $NaYF_4:Yb^{3+}$, Tm^{3+} nanophosphors and designated as UPCN_M. Briefly, 10 g of *M. oleifera* fresh mature leaves, collected from the Botanical garden of Banaras Hindu University, were washed thoroughly in deionized water (18 M Ω cm^{-1}) and dried at room temperature. The leaves were boiled at ~90 ^oC for 4h in 100 mL DI water in a tightly closed beaker. The resulting solution was filtered through Whatman#1 filter paper to remove any solid impurities. Briefly, 0.2 M stock solution of YCl_3 (99.99%, Otto and Himedia Chemicals, India), $YbCl_3$ (99.99%, Otto and Himedia Chemicals, India) and $TmCl_3$ (99.99%, Sigma Aldrich, India) all are in its hydrated form, were prepared by dissolving individually in leaf extract as well as in DI water as solvent. Additionally during aqueous phase (DI water) synthesis of Upconverting phosphors ethylenediaminetetraacetic acid (EDTA) employed as a chelating agent. UPCN synthesized from *M.oleifera* extract and (deionized water-EDTA) termed as UPCN_M and UPCN_EDTA respectively throughout the manuscript. In a typical synthesis 0.83 M of NaF (99.99%, SRL Chemicals, India) stock solution was prepared in both leaf extract as well as DI water. 30 mL of suspension was prepared by magnetically stirring 75.4 % of NaF, 20 % Y^{3+}, 3. 77 % Yb^{3+} and 0.75 % Tm^{3+} both in organic as well as DI water media. Mixture was then transferred to a Teflon lined stainless steel autoclave and heated to 215 ^oC under continuous stirring (hot plate with magnetic stirrer) for 2h, 5h and 15h respectively. After completion of reaction, the autoclave was cooled down to room temperature and suspended particulates were separated as well as

washed by repetitive centrifugation and sonication in ethanol and DI water. Then collected UPCN crystals were dried overnight in an oven at 60 ^{o}C and stored.

5.2.2 Characterizations

X-Ray Diffraction (XRD) studied were carried out with the help of Rigaku Smart Lab diffractometer using CuK_{α} radiation source. Surface morphology, topography and size was studied with the help of Scanning electron microscopy (FEI NOVA NANOSEM 450), transmission electron microscopy (FEI TECNAI G^2 20 TWIN). Selected area diffraction (SAED) pattern also recorded in the same transmission electron microscope. Presence of organic functional groups was investigated using FTIR spectroscopy (Perkin Elmer L1280044).

Synthesized UPCN was characterized for luminescence emission using spectrofluorometer, (PTI, Quanta Master 400 USA) equipped with S-171 photon multiplier tube (PMT, R928P). Fluorescence studies were carried out using constant wave near infrared laser (MD-III-975-2W) with 2.6 nm slit opening and step size of 1 nm, and integration time of 0.1 sec. The absorbance studies were carried out with the help of Carry 60 UV-Visible spectrophotometer (Agilent Technologies, India Pvt. Ltd.) The magnetization studies on powder compacts were carried out with the help of MPMS magnetometer (VSM Quanta Design). Field dependent magnetization behavior of sample was investigated at constant temperature of 2K and 300K with varying magnetic field of ± 7T.

5.2.3 Photothermal Heat Generation & Dissipation by UPCN_M on NIR Exposure

Heat generation and dissipation capability of UPCN_M under ~975 nm laser (MDL-III-2W) excitation was evaluated as a function of exposure time. In a typical experiment, 0.5 and 0.1 mg/mL of UPCN_M suspension in DI water were exposed to NIR light and

temperature rise with time was monitored by a K-type thermocouple connected with a digital indicator (DTI-537, Senstec Thermal controls). Temperature rise and cooling in case of *M.oleifera* leaf extract as well as DI water also monitored under similar conditions.

5.3 Results and Discussion

One of the major goals of the current study is to evaluate phase transformation, change in morphology and other physical properties of the Upconverting nanophosphor (UPCN), when *M.oleifera* leaf extract is used as synthesis medium. Therefore, a fixed reaction temperature of ~215 ºC, and processing time of 2, 5 and 15h was chosen for the UPCN_M synthesis. Conventionally Upconverting nanophosphors have been synthesized using EDTA as a chelating agent and have been well studied [357, 358]. Therefore, for comparison, the Upconverting nanophosphors were also synthesized using EDTA as chelating agent (UPCN_EDTA). The crystallographic phase formation in the Upconverting nanophosphors synthesized using leaf extract EDTA was evaluated by XRD (Fig. 5.1). The XRD pattern of UPCN_M with 2h processing time, largely matches with the standard XRD pattern of hexagonal β-$NaYF_4$ (JCPDF Card No. 98-007-6718). On longer processing times (5h), the β phase started to transform into the cubic α-phase. As a result, the peaks (2θ: 29.9, 30.7, 43.4°) corresponding to β-$NaYF_4$ displayed reduced intensity and slightly shifted to the higher 2θ values, indicating slight reduction in lattice parameters. While, low intensity peaks (at 2θ: 28.26°, 46.68°) corresponding to the cubic α-$NaYF_4$ (JCPDF Card No. 98-001-9092) could be observed. The intensity of all the XRD peaks belonging to both α and β phases were lower and slightly shifted. This could be due to formation of the transient phase. The XRD of the 5h processed sample is depicted in figure 5.1a. In addition to the peaks corresponding to α and β $NaYF_4$, three

more peaks at 2θ: 38.88, 56.1 and 70.32° appeared in the 5h processed samples, which matched with the standard pattern of NaF (JCPDF Card No. 98-004-8929). On increasing the processing time to 15h, the intensity of the XRD peaks belonging to the α-$NaYF_4$ increased, while peaks belonging to the β-phase disappeared. Additionally, the extra peaks at 2θ: 38.88, 56.1 and 70.32° corresponding to NaF remained intact.

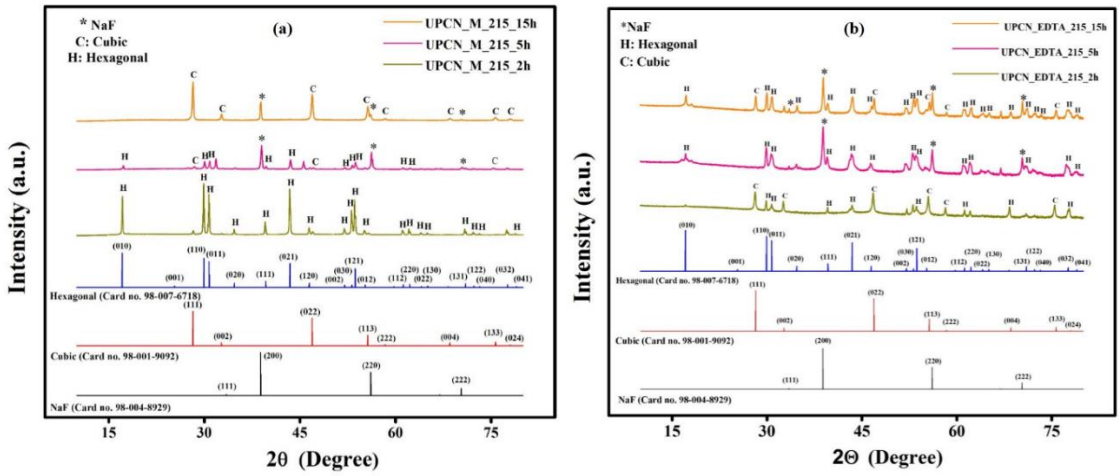

Figure 5.1 Powder x-ray diffraction pattern of UPCN_M (a) and UPCN_EDTA (b) synthesized at 2h, 5h and 15h.

This indicated that 2h processing, results in the formation phase pure β-$NaYF_4$, which, on longer processing time, starts transforming to the α-$NaYF_4$ with concomitant appearance of NaF peaks. It is noted that no peak corresponding to the YF_3 is observed at any stage of synthesis, suggesting precipitation of excess NaF from and not as decomposition product. It is important to note that during processing, 15% extra NaF was added to compensate for losses during longer processing times (> 2h).

The precipitation of NaF from the solution results in appearance of a very faint peak at 2θ ~39°, as observed in 2h processed samples. The peaks corresponding to NaF increased in intensity with time and by 5h the precipitation of NaF was complete. As a result, not much change in the intensity of XRD peaks at 2θ: 38.88 and 56.1° is observed on

processing beyond 5h. Therefore, XRD peaks corresponding to NaF appeared due to the precipitation of extra NaF dissolved in solution. It is interesting to observe that β-$NaYF_4$ to α-$NaYF_4$ transformation could take place at a much low-temperature (215 °C) in this case, which otherwise have been reported to happen at much higher temperatures (above 600 °C) [359]. Using this green processing route, β-$NaYF_4$ Upconverting nanophosphors is synthesized at a much lower temperature (~215 °C) and displayed comparatively faster phase transformation.

It is important to note that the presence of various organic ligands (examined by GC-MS, FTIR analysis, shown later) may also have involved in the rapid phase transformation of the UPCN, by reducing the interfacial energy of the developing phases. On the other hand, the XRD analysis of UPCN_EDTA sample (Fig. 5.1b) showed a mixture of α and β phase, for the sample synthesized at 2h. This sample on further processing (5h reaction time), converted to β phase, largely and concomitantly, intense NaF peak also appeared. While on processing for 15h, again a mixture of α and β phase was observed along with appearance of NaF. This is in contrast to the samples prepared using *M. oleifera* leaf extract, where mostly β, mixture of α and β and largely α-phase was obtained at 2h, 5h, and 15h processing time, respectively. It was noticed that use of leaf extract, somehow accelerates the rate of phase transformation in the $NaYF_4$ system.

To compare the phase changes in both the cases (*M. oleifera* and EDTA) the intensity ratio of the highest peaks of α and β-$NaYF_4$ was plotted as function of processing time (Figure 5.2). It can be observed that in the case of *M. oleifera* as reaction medium, the I_β (Intensity of (021) XRD peak of β-phase) was about 7 times more intense than the I_α (Intensity of (111) XRD peak of α-phase) for 2h processed sample, which reduced progressively to zero for 15 h synthesized sample. On the other hand, in the case of

UPCN_EDTA, the intensity ratio I_β/I_α was about 0.8 for 2h, which increased to ~10 for 5h processing time and then reduced back to 2 for 15h processed samples. This indicates that in the case of EDTA processed sample, larger amounts of alpha phase (almost 2 times to that of β-phase) was present in the 2h processed sample, reduced to almost 0.5 times on 15h processing. In contrast, UPCN_M (*M.oleifera* assisted synthesis) not only crystallized into β phase in 2h, but also started β→α transformation much earlier and ultimately converting to pure α phase in 15h.

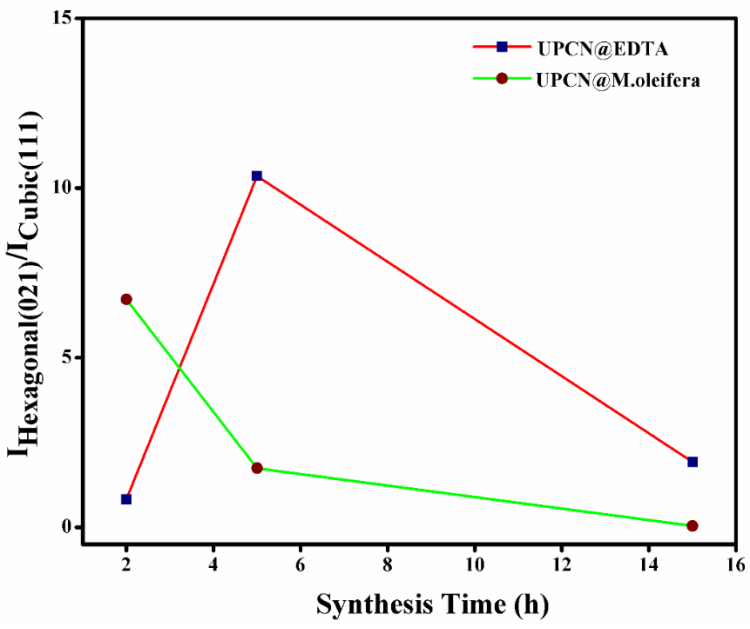

Figure 5.2 Quantification of transition of hexagonal phase with respect to cubic phase

The *M.oleifera* extract contains several organic ligands such as 3-hydroxy butanoic acid, linoleic acid, palmitic acid and gamma tocopherol, catechol, which can preferentially attach to certain crystallographic planes and influence the developing facets of UPCN during synthesis. From the leaf extract analysis by gas chromatography-mass spectroscopy (GC-MS), presence of these ligands has been confirmed as shown in figure 5.3.

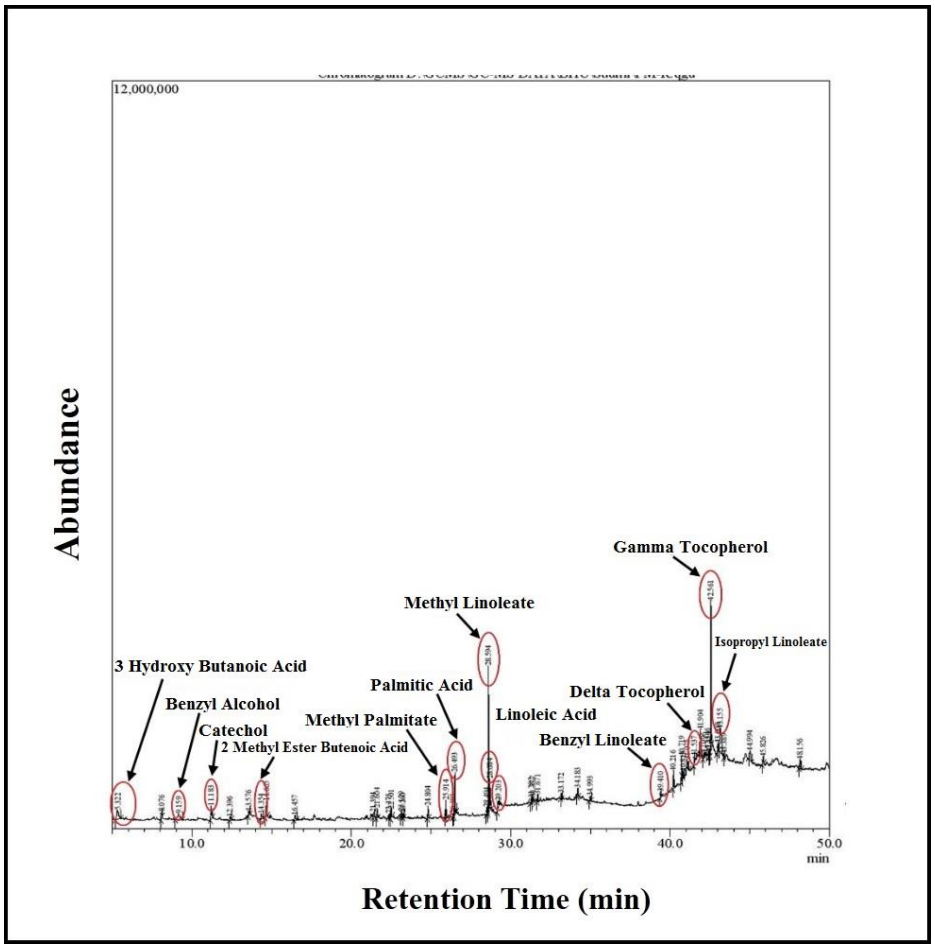

Figure 5.3 GC-MS of *M.oleifera* leaf extract showing presence various organic molecules and their abundance.

Similar observation has also been made earlier where citric acid was used as chelating/capping agent in the synthesis of Upconverting phosphors [177, 203]. The effect of *M.oleifera* leaf extract on the UPCN_M morphology and size was also evaluated using scanning electron microscopy shown in *Appendix* C1. The increasing processing time from 2h to 5h resulted in substantial increase in particulate size from ~150 nm (*Appendix* C2a) to roughly micrometer dimension (*Appendix* C1b). However, on longer processing time to 15h, particle size decreased to ~114 nm (*Appendix* C2b). This initial increase in particulate size may occur due to coalescence and grain growth with time. However, further processing for longer times resulted in much smaller particles. This

could be rationalized by nucleation of α-phase within β-phase particles which can induce strain within the larger β-phase particles which leads to breaking down of particles during the transformation and results in much smaller α-phase particles. Further the UPCN_M morphology was investigated using the transmission electron microscopy (Fig. 5.4).

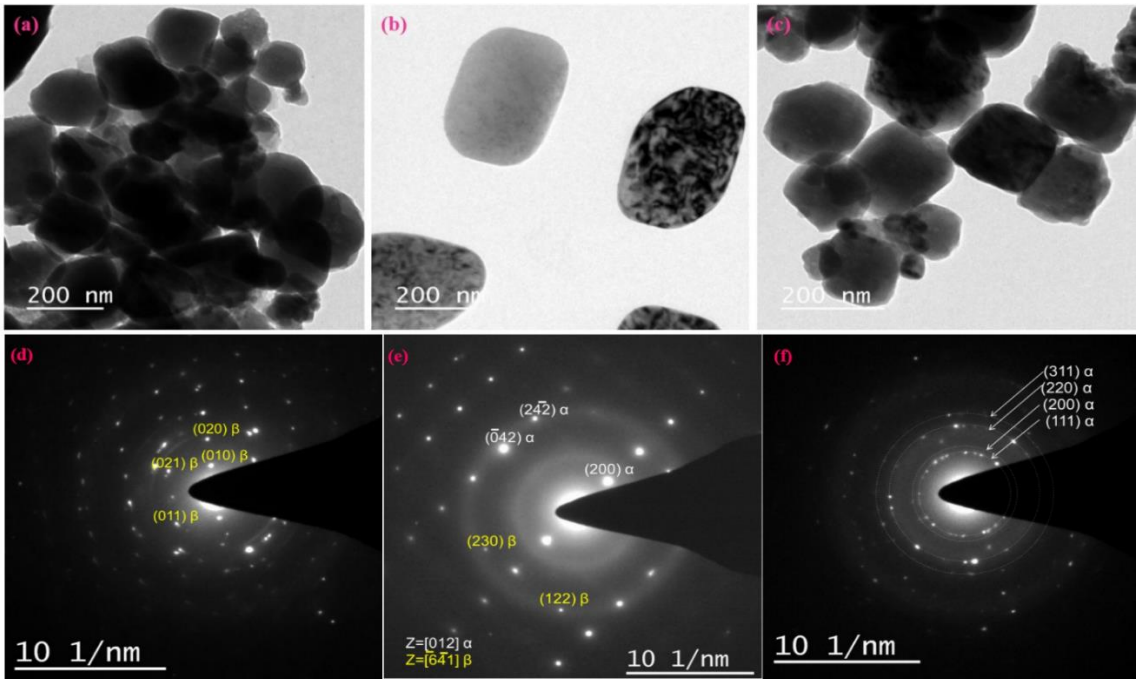

Figure 5.4 TEM images of UPCN synthesized at (a) 2h (b)5h and (c)15h. For the same samples SAED acquired for UPCN_M synthesized at (d) 2h (e) 5h and (f) 15h.

The TEM images of UPCN_M clearly show formation of particles of ~100 nm to 150 nm (Fig. 5.4a) in size on 2h processing. On increasing the processing time to 15h, agglomerated particles having much smaller sizes were observed (Fig. 5.4c). On the other hand, TEM bright field image of 5h (Fig. 5.4b) processed UPCN_M particles were larger in size. However, the particles did not have uniform contrast, and dark spots were observed in bright field (BF) images. This contrast could be due to diffraction from the cubic phase, nucleating with in the well grown larger β-phase. The diffraction pattern of the 2h processed sample could be indexed to pure β-phase (Fig. 5.4d), on the other hand, the diffraction pattern of the 5h processed sample contained spots from both β and α-

phases which could be independently indexed (Fig. 5.4e). This resulted in breaking down of UPCN during transforming into the smaller stable α-phase nanoparticles. The 15 h processed samples had ring like pattern which could be indexed to the cubic phase (Fig. 5.4f). This observation further confirmed that the β→α phase transformation begins with in the β particles, which during transformation into α phase break down into smaller particle. These observations were in line with the observations made through XRD and SEM. It has been reported earlier that a structural orientation relation $[110]\alpha//[110]\beta$ and $\{002\}\alpha//\{2\bar{2}0\}\beta$ exists as represented in figure 5, which can facilitate nucleation of α phase within the β particles [355, 359].

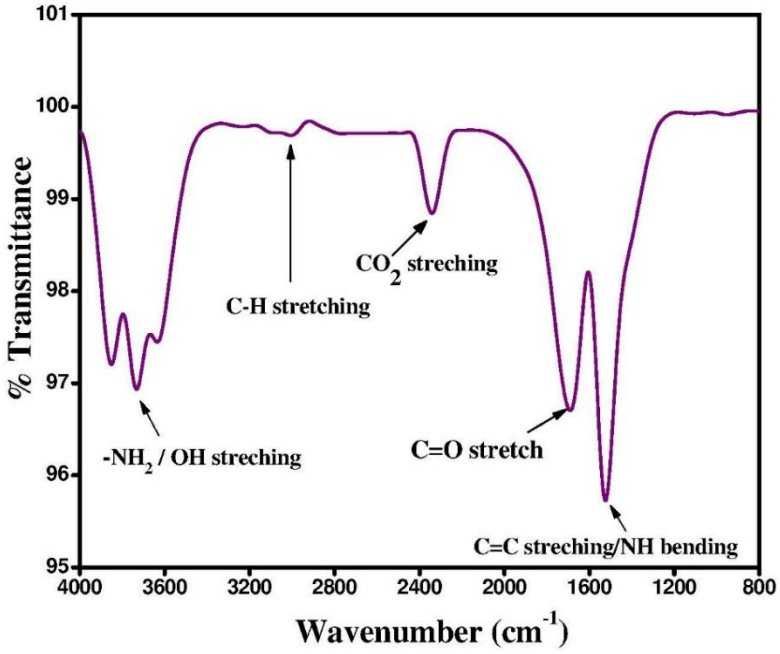

Figure 5.5 FTIR spectroscopy of UPCN synthesized from *M. oleifera*

Notice that non-radiative losses occurs through the high energy vibrational modes (4000-1000 cm^{-1}). Therefore, Fourier transform infrared spectroscopy (FTIR) of UPCN_M was acquired and shown in figure 5.5. The FTIR data indicated fairly sharp vibrational bands at wavenumbers ~ 1520, 1690, 2340, 3000 cm^{-1} and in between 3600-3850 $cm.^{-1}$

Appearance of ~1520 cm^{-1} band can be attributed to C=C stretching of the alkene group, while ~1690 cm^{-1}could have resulted from C=O stretching of carbonyl/aldehyde/ester functional groups. The band at 2340 cm^{-1} may have resulted from carbonate contamination arising from decomposition of organic precursor during hydrothermal synthesis [225]. Apart from this it may correspond to thiocyanate or isothiocyante functional groups resulted from cleavage of glucosinolate compounds in presence of water. Slight transmittance peak near 3000 cm^{-1} is mainly due to CH/OH stretching vibrations of carboxylic acid, alcohol and alkene functional groups. The transmittance spectra in between 3600-3850 cm^{-1} could be attributed to the NH_2/OH-stretching of phenolic/alcoholic/amine groups present in *M.oleifera* leaf extract. Since, *M. oleifera* consists of several proteins and amino acids [226, 228, 230], hence primary amine vibrations can be seen at higher wavenumbers. Presence of entire spectra of functional groups discussed above can be correlated with the organic compounds detected from gas chromatography-mass spectrometry (GC-MS) analysis of leaf extract. Interestingly, the presence of carbonyl and hydroxyl functional groups are most likely to have resulted from polyphenolic compounds (e.g. catechol), a well-known reducing agent, present in the *M.oleifera* leaf extract, also detected by GC-MS (Fig. 5.3). Similarly, combination of carbonyl, hydroxyl, alkyl as well as alkene stretching results from the long-chain fatty acid compounds in *M. oleifera* leaf extract (linoleic acid, palmitic acids, gamma and beta tocopherol) playing an important role in nucleation, growth and stabilization of UPCN_M [230].

The effect of aforementioned ligands on Upconverted emission of the UPCN_M powder was evaluated under 975 nm light excitation as shown in figure 5.6. Upconverted emission intensity of UPCN_EDTA also recorded under the 975 nm laser excitation. Both the phosphors (UPCN_M and UPCN_EDTA) displayed same emission bands under ~975

nm light excitation. The luminescence data (Fig. 5.6a) revealed emission at 345, 360, 450, 478, 645, 700 and 800 nm (*Appendix* C4) due to $^3P_0 \rightarrow {}^3H_4$, $^1D_2 \rightarrow {}^3H_6$, $^1D_2 \rightarrow {}^3F_4$, $^1G_4 \rightarrow {}^3H_6$, $^1G_4 \rightarrow {}^3F_4$ and $^3F_3 \rightarrow {}^3H_6$, $^3H_4 \rightarrow {}^3H_6$ electronic transitions respectively, confirming Upconversion process.

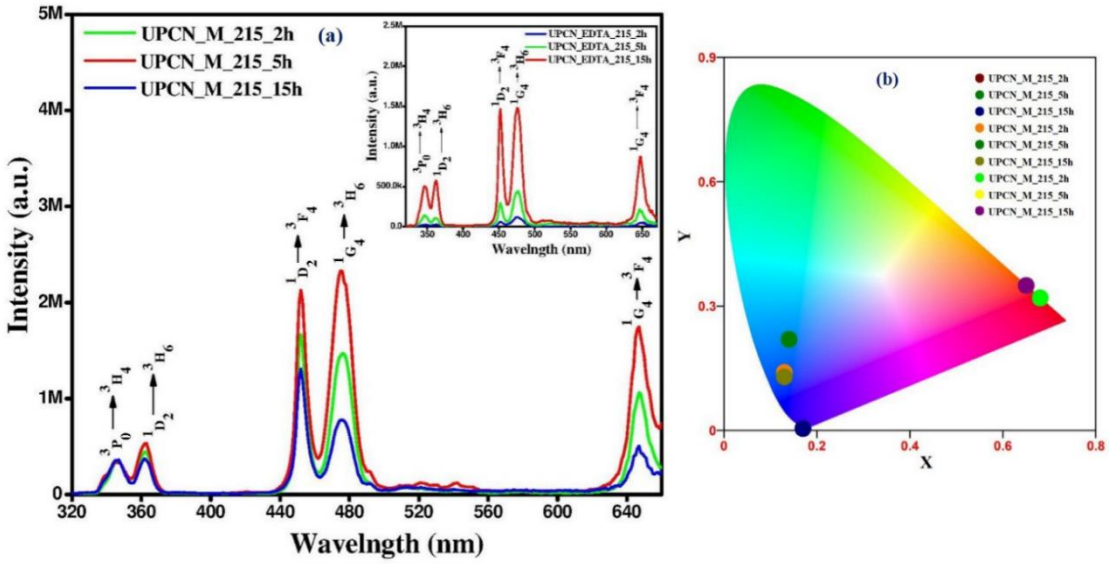

Figure 5.6 (a) Comparative emission analysis of UPCN synthesized from *M. oleifera* (Main figure) and EDTA assisted aqueous medium (inset) for different time interval (b) CIE diagram indicating colour coordinates for Upconverted emission at different time duration

It is important to notice that the relative intensities of different bands within the spectrum varied substantially. The emission intensities resulting from UPCN_M processed for 2h and 15h were in decremented order, while that processed for 5h abruptly displayed strongest emission. It is observed that in the case of 2h processed UPCN_M samples, β-phase predominates, known to display better Upconverted emission. At the same time 15h samples rich in α-phase, predictively displayed lower emission intensity as compared to 2h processed sample. While, 5h sample exhibited mixed phase and showed unusually high emission intensity. The XRD and TEM images revealed the nucleation of α-phase

with in the β particles which could result in strained crystals leading to enhanced emission intensity [360-362].

Interestingly, UPCN_EDTA sample displayed progressively increasing Upconverted emission with processing time. Notice that processed UPCN_EDTA sample exhibited mixed α and β phase, which varied with processing time. The 2h processed sample displayed lowest β content and hence displayed minimum emission intensity, while The 5h sample with high β-content displayed slightly better emission as compared to 2h samples. It is important to note that relative intensity of XRD peaks corresponding to the β phase in the 5h processed samples were much lower, indicating poor β-phase crystallization. The β-phase was well crystallized (as reflected by I_β/I_α ~2) after 15h processing. The presence of larger fraction of well crystallized β phase resulting in efficient Upconverted emission from 15h samples as compared to 5h samples. The luminescence data revealed that relative emission intensities from UPCN_EDTA and UPCN_M differed from each other under 975 nm excitation. The emission intensity in the case of UPCN_EDTA was found to be low as compared to those samples prepared with *M. oleifera*. Even maximum emission intensity achieved by 15h sample, was comparable or slightly lower than UPCN_M sample prepared in 2h. This observation is likely due to the rapid phase transformation in the case of leaf extract, where hexagonal phase is the dominant phase during 2h of synthesis. Whereas, maximum intensity observed from UPCN_EDTA_15h samples, due to delayed phase transformation, from cubic to hexagonal in it. The above results support the advantage of using *M.oleifera* leaf extract as probable nucleating and stabilizing agent to obtain better emission intensity. Moreover, comparative study indicated better overall Upconverted emission intensities from UPCN_M as compared to UPCN_EDTA, known to contain $-NH_2$ groups and play important role in enhanced Upconverted intensity [363].

The emission from UPCN_M was mapped to the colour chromaticity (CIE) diagram. The CIE (international commission for illumination) diagram provides an insight into the different colours generated from the synthesized samples. To get a perspective of different colour emission from phosphors processed for different time periods, CIE coordinates were calculated (Fig. 5.6b). Figure 5.6b shows that violet emission remained constant regardless of processing time, while other colours such as green and red are clearly demarcated. The slight green Upconverted emission also has some interference effect during colour coordinate calculation. The non-radiative energy losses in case of UPCN result into photothermal heat generation, which can be employed in the treatment of cancer and tumor. Therefore, capability of UPCN_M to generate heat under 975 nm excitation was evaluated and shown in figure 5.7.

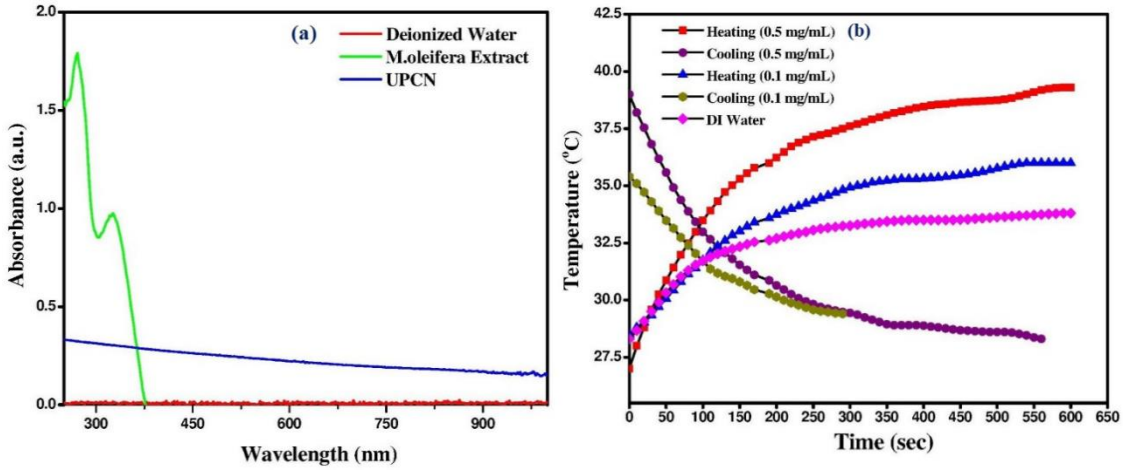

Figure 5.7 (a) Absorption spectra of UPCN as compared to deionized water and *M. oleifera* leaf extract. (b) Heating and cooling profile of UPCN prepared from *M.oleifera* in powder and in suspension form upon NIR Excitation.

From the absorption spectra (Fig. 5.7a) it is clearly identified that absorption has no significant role in generating photo thermal heat upon NIR exposure. In fact, UPCN has better NIR absorbing capability as compared to deionized water and *M. oleifera* leaf extract in terms of absorption intensity. However, the heat generation in the present case

of UPCN_M may be attributed to non-radiative relaxation process during Upconversion process.

Thulium-doped Upconverting phosphors have been previously used in various biomedical applications such as photothermal therapy [364]. During Upconversion process large fraction of photon energy is converted into heat energy. This heat energy can be used for killing the cancer cells. Besides, use of 975 nm laser as a radiation source for heat generation from UPCN_M, facilitates penetration through deep tissue and hence, such therapies have higher chance to succeed in practical terms. Therefore to ascertain UPCN_M potential to generate sufficient heat to kill such cells is studied using 500 mW NIR laser. Studies were performed on UPCN_M suspension in DI water for 10 min exposure time (Fig. 5.7b). Before heating experiment on UPCN_M suspension, DI water was exposed to NIR laser for 10 min and temperature rise was recorded. There was only 5 degree (28 ^{o}C to 33 ^{o}C) temperature rise in 10 min. In case of 0.1 mg/mL and 0.5 mg/mL UPCN_M suspension in DI water temperature change (ΔT) was found to be 8.5 and 11.5 ^{o}C respectively for the same exposure time, indicating photothermal heat generation rate of 0.85 ^{o}C/min and 1.15 ^{o}C/min respectively (Fig. 5.7b). Specifically, the photothermal conversion efficiency (η) of this green synthesized UPCN is calculated to be ~3% (*Appendix* C3). As per earlier reports by Liu et al. [365], in the case of $NaYF_4$: Yb, Er@$NaYF_4$: Yb coated with polydopamine (PDA), a heating rate of 1 ^{o}C/min was observed upon exposure to 808 nm laser. However, it is important to note that in that case PDA was used to enhance the NIR absorption and transduction, although in current studies, no external NIR absorbing entities were used. Moreover in our case, UPCN_M suspension concentration is physiologically relevant for biological studies [366, 367]. Certainly, this study demonstrate that leaf extract of *M.oleifera* has played important role in photothermal heat generation comparable to the published reports.

Further application in the field of MRI contrasting agent and magnetic separation etc. requires detailed study regarding magnetic properties of UPCN_M. Combined effect of deposited organic ligands on surface of UPCN_M as well as shape or size anisotropy and crystallinity may influence the magnetic behavior [368], hence it should be thoroughly examined. To study the effect of aforementioned parameters on magnetic property, field dependent magnetization studies of UPCN_M was carried out through MPMS technique. Magnetic properties were measured at 2K and 300K in the field range of ± 7T as shown in figure 5.8. The cryogenic studies display excellent super-paramagnetic behavior in UPCN_M (2, 5 and 15h) at higher field range (Fig. 5.8a). UPCN_M synthesized for 2h has the highest magnetic saturation among its other two counterparts produced at 5h and 15h having magnetic saturation 10.2, 5.8, 7.6 emu/g respectively (Fig. 5.8a).

Magnetic spins of constituent atoms aligned in a same direction at low-temperature resulting S shaped magnetization curve. Decrease in magnetic saturation value at higher residence time may be due to quenching of magnetic moment resulting from interaction of deposited diamagnetic organic ligands with UPCN [369]. Apart from this surface contribution, surface

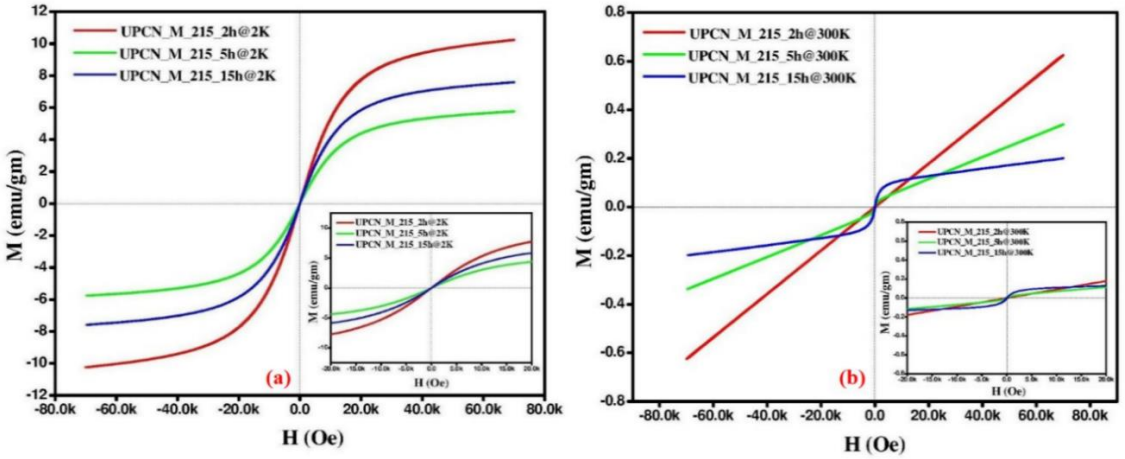

Figure 5.8 Magnetic property measurement study of Upconverting nanophosphors synthesized using *M.oleifera.* Field dependent magnetization curve of UPCN_M

measured at 2K (a) and 300 K (b). Inset image in both the figures showing magnified image at lower applied field.

disorder and effect of adsorbed water may be another factor as reported by kombaiah et al. [368]. But when the higher field magnetization curve is extrapolated to lower field range, paramagnetic or weak super-paramagnetism nature clearly visible pertaining to its linear MH curve having negligible hysteresis [370]. Room temperature field dependent magnetization data, UPCN_M (Fig. 5.8b) also displayed the same pattern of magnetism. The data basically showing formation of paramagnetic UPCN_M as a result of very narrow hysteresis curve with nearly zero corecivity value. Moreover, magnetic property of 5h prepared UPCN_M showing very weaker super-paramagnetism due to its abnormal crystallinity and overcoming of the anisotropy energy barrier by thermal energy. Discrepancy in magnetic behaviour is expected in the current case due to absence of any kind of clear cut magnetic domain in Upconverting system as compared to conventional magnetic nanoparticles. Paramagnetic as well as super-paramagnetic values of UPCN_M at room temperature as well as cryogenic temperature are found to be insignificant for any application in the area of magnetic resonance imaging or magnetic separation. Though magnetization results are encouraging but due to uncommon phenomena in Upconverting systems it must be properly investigated for further improvement prior to its application.

5.4 Conclusion

$NaYF_4$: Yb^{3+}, Tm^{3+} UPCN were successfully synthesized using *M.oleifera* leaf extract. It was demonstrated that use of leaf extract resulted in the formation of nearly phase pure β-$NaYF_4$ at a lower processing time (2h) unlike EDTA assisted synthesis where transition from cubic to hexagonal phase occurred at high processing time (15h). Even maximum

emission intensity achieved at 15h synthesis condition, in case of UPCN_M was comparable or slightly lower than UPCN emission intensity synthesized from *M. oleifera* at 2h processing time. Similarly use of *M.oleifera* in synthesis resulted in improved red emission. Under 975 nm excitation, in physiologically relevant concentration, UPCN_M (0.5 mg/mL) displayed the heating rate of 1.15 ^{o}C/min. The cryogenic studies displayed excellent super-paramagnetic behavior in UPCN_M (2, 5 and 15h) at higher field range with magnetic saturation value achieved as 10.2, 5.8, 7.6 emu/g respectively. Also UPCN_M showed room temperature paramagnetism. In essences, our studies demonstrates improvement in some of the intrinsic properties of UPCN_M due to use of *M.oleifera* leaf extract.